ACS OMEGA

http://pubs.acs.org/journal/acsodf

Article

Highly Selective Electrochemical Synthesis of Urea Derivatives Initiated from Oxygen Reduction in Ionic Liquids

Erin Witherspoon, Pinghua Ling, William Winchester, Qi Zhao, Ahmad Ibrahim, Kevin E. Riley, and Zhe Wang*

Cite This: *ACS Omega* 2022, 7, 42828−42834

Read Online

ACCESS | Metrics & More | Article Recommendations | Supporting Information

ABSTRACT: The development of more efficient and sustainable methods for synthesizing substituted urea compounds and directly utilizing CO_2 has long been a major focus of synthetic organic chemistry as these compounds serve critical environmental and industrial roles. Herein, we report a green approach to forming the urea compounds directly from CO_2 gas and primary amines, triggered by oxygen electroreduction in ionic liquids (ILs). These reactions were carried out under mild conditions, at very low potentials, and achieved high conversion rates. The fact that O_2 gas was utilized as the sole catalyst in this electrochemical loop, without additional reagents, is a significant milestone for eco-friendly syntheses of C−N compounds and establishes an effective and green CO_2 scavenging method.

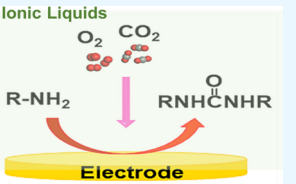

INTRODUCTION

Currently, about 3.54 billion people globally are fed by synthetic nitrogen fertilizers, over 70% of which are composed of urea and its derivatives. Demand is expected to increase even further as the population continues to grow.[1,2] Moreover, as an important class of carbonyl compounds and valuable chemical intermediates, urea derivatives are widely used in pharmaceuticals, textiles, medicine, and other agricultural chemicals.[3−5] They are also used as dyes, energy carriers, antioxidants, corrosion inhibitors, and additives in plastics.[6−9] Presently, the conventional production of urea is accomplished through the reaction of NH_3/RNH_2 and CO_2.[10,11] This synthesis is generally described in Scheme 1.

Scheme 1. The Conventional Production of Urea through the Reaction of NH_3/RNH_2 and CO_2

$$2RNH_2 + CO_2 \overset{(1)}{\rightleftharpoons} R\text{-}NH\text{-}CO_2^-NH_3^+\text{-}R \xrightarrow{(2)} (R\text{-}NH_2)_2\text{-}CO + H_2O$$

The standard Gibbs free energy changes for reactions (1) and (2) are −23.8 and +16.7 kJ, respectively, at 25 °C and 1 bar. As a kinetically slow process, reaction (2) is thermodynamically infeasible at the ambiance; thus, significant external energy and catalysts are needed.[12] This reaction is initiated from the carbamate salt form, at which point the amine group is required to nucleophilically attack the carbonyl group. Strong bases such as CsOH, Cs_2CO_3, KOH, and [BMIM]OH are utilized in the chemical process to generate negatively charged R-NH^- or R-NH* radical. However, their reactions with CO_2 limit the production efficiency when using CO_2 gas directly. Thus, current methods are energy-intensive (150−200 °C, 150−250 bar), with production costs being ∼2% of annual global energy.[13] Dangerous reagents such as phosgene and isocyanates and multicycle processes are also required to improve the conversion efficiency.[14]

Using renewable electrical energy to synthesize urea derivatives is considered as a promising green alternative for next-generation industrial production.[15,16] The C−N structure has previously been generated by activating the linear form of CO_2 to CO_2^- by applying overpotentials of about −1.9 V, but temperatures of 100−200 °C were still required.[17−24] Further, Xia's group used −15 kV of the negative corona to ionize NH_3 and CO_2 gases to form urea at 1 bar and 20 °C, achieving 82% CO_2 conversion and 51% urea selectivity.[25] In aqueous solutions, Wang and Li's group investigated the coupling CO_2 and N_2 electrochemical reduction on metal-based catalyst surfaces. A faradaic efficiency (FE) of 8.92% was reported on PdCu and TiO_2 catalysts.[14] Both mechanisms involved COOH* as a key electrochemical intermediate from CO_2. To avoid the high dissociation energy of N_2 triple bonds (941 kJ/mol) and the limited solubility of N_2 in H_2O (0.02 v/v, 25 °C, 1 bar), nitrite solutions were used as feedstock with efficiencies of about 25−55% on different gas-diffusion metal electrodes.[26,27] However, conventional precious metal-based alloy catalysts suffer from ambiguous active sites and easy corrosion.[15,28,29] In the electrochemical approach, the co-reduction reactions achieved on metal-based catalysts could increase the conversion through a possible coupling pathway of NH_2* and COOH* intermediates for urea formation. Accordingly, the solubility of ammonia and CO_2 play a key

Received: July 27, 2022
Accepted: October 18, 2022
Published: November 15, 2022

role in conversion efficiency.[30] Other limiting factors include the high overpotential of the CO_2 reduction and the hydrogen evolution reaction involved in aqueous solutions.

We believe that this synthesis could be improved further by using green and readily available materials under milder conditions. Ionic liquids (ILs) are novel green solvents used in many chemical and electrochemical reactions.[31,32] Here, hydrophobic ILs are used as electrolytes/solvents for urea formation directly from CO_2 and amines since they are inert toward all compounds involved in the reaction and CO_2 is highly soluble in the solvents. Our group has completed extensive work on electrochemical reactions in ILs.[33−35] As reported, strong nucleophiles, superoxide and peroxide ions, generated through the electrochemical reduction of oxygen, could be even more stable in ILs than in traditional aprotic solvents (i.e., DMSO and acetonitrile) and participate in several organic reactions in completely green processes.[36,37]

In this work, we hypothesize that active oxygen ions (or reactive oxygen species (ROS)) could activate various amines and further enable the nucleophilic attack of carbamate salts. It is well known that at room temperature and even at low pressure, CO_2 quickly reacts with amines in the first step of the chemical synthesis process, reaction (1). The linear structure of CO_2 becomes bent to carbamate acid or carbamate anion, and the exposed nucleophilic site of carbon could effectively react with R-NH^- or R-NH* nucleophiles. Thus, the recovered ammonium salts could be directly converted into urea with less additional energy input, which is a more practical industrial approach and an efficient ammonia-recovery method. Herein, the reactions were evaluated under ambient temperature and pressure in both protic and aprotic ILs, without catalysts, to provide potential adaptability and universality of this method. Cyclic voltammetry (CV), theoretical density functional theory (DFT) calculations, and in situ Fourier transform infrared (FTIR) spectroscopy were conducted to understand the reaction mechanisms and possible pathways.

MATERIALS AND METHODS

Materials. Carbon dioxide (99.99%) and oxygen (99.99%) were purchased from Airgas, Inc. All amines, deuterated solvents, and sodium peroxide (95%) were obtained from Fisher Scientific. ILs were from IoLiTec Ionic Liquids Technologies GmbH. All chemicals were used as received without further purification. The nuclear magnetic resonance (NMR) spectra were recorded using a Bruker Avance 300 spectrometer and were calibrated using residual undeuterated solvent as an internal reference ($CDCl_3$, 77.16 ppm ^{13}C NMR; C_2D_6OS, 35.92 ppm ^{13}C, 2.50 ppm ^1H NMR). The FTIR absorption spectra were recorded on a Varian 3100 Excalibur Series spectrometer in the region of 400−2000 cm^{-1} using two NaCl disks also from Fisher Scientific for non-in situ measurements. The electrochemical tests were performed with a CHI660E electrochemical analyzer with platinum wire as the reference and counter electrodes and a gold plate as the working electrode.

Preparation of C−N Organic Compounds. 700 μL of 1-butyl-1-methylimidazolium bis(trifluoromethylsulfonyl)-imide ([BMIM] [NTf_2]) or 1-butyl-1-methylpyrrolidinium bis-(trifluoromethylsulfonyl)-imide ([BMPyrr] [NTf_2]) (Figure S1) was loaded in a Teflon cell then CO_2 (50 sccm) and O_2 (20 sccm) were bubbled in for 30 min. The mixture was reacted at −1.9 V for another 30 min. Finally, 300 μL of the selected amine was added into the cell, and the reaction continued for another 5 h at −1.9 V. For reactions using [BMPyrr] [NTf_2], −1.7 V was applied. For generation using Na_2O_2, 700 μL of [BMPyrr] [NTf_2] was added to 300 μL of CHA, and then CO_2 was purged through the mixture for ∼1 min. Next, ∼0.250 g of Na_2O_2 was added, and the mixture was shaken for ∼1 min, and subsequently, CO_2 was purged for ∼1 min more. The final reaction mixtures were vacuum filtered and washed with acetone.

Cyclic Voltammetry Measurements. CV measurements were completed using the same electrochemical cell and setup; however, only 50 μL of CHA was added in this case to avoid buildup of the solid product, and rather than constant potential, the potential was swept between 0.5 and −2.0 V. In addition, step 1, the salt formation step, took place outside the cell, and a specific mass (0.5 g) was added subsequently. CVs were scanned at 200 mV/s for 8 cycles.

In Situ Fourier Transform Infrared Spectroscopy. In situ EC-FTIR measurements were recorded using a Bio-Logic Thin Layer Spectroelectrochemical Cell with a gold gauze working electrode, a platinum gauze counter electrode, and a platinum wire reference electrode, with [BMIM] [NTf_2] as the electrolyte. A constant potential of −1.9 V was applied continuously to the cell for over 7 h; O_2 gas was purged for the same duration. The spectra were recorded every 10 min with 20 scans and a sensitivity of 1.

^{13}C Isotope Nuclear Magnetic Resonance Spectroscopy Characterizations. A Bruker 200 MHz NMR spectrometer was used to record ^{13}C isotope products using ^{13}C NMR. Both the ^{13}C salt product and ^{13}C urea product were prepared using the same technique as ^{12}C products but substituting $^{12}CO_2$ with $^{13}CO_2$, supplied from Sigma-Aldrich (99.0%). In this case, a magnetic stir bar was added to the reaction vessel since the $^{13}CO_2$ gas was a low-pressure gas incapable of bubbling into the mixture. The reaction was stirred at room temperature for 15 min before collecting the NMR spectrum.

Computations. DFT computations were carried out at the PW6B95/def2-TZVP level of theory and utilized the SMD implicit solvation model (ε = 10) to mimic the IL environment. All calculations were carried out using the Gaussian G16 suite of molecular electronic structure programs. All structural optimizations were carried out using "tight" convergence criteria. Thermal corrections used to compute Gibbs energies for products, reactants, and intermediates were computed using harmonic vibrational analysis.

RESULTS AND DISCUSSION

To investigate the reaction between activated O_2 and the carbamate salt formed in step 1 (Scheme 1), a three-electrode system was used to study the electrochemical process between CO_2/cyclohexylamine (CHA) salt and ROS in [BMIM] [NTf_2]. Figure 1 (black curve) shows a typical CV curve of the two-step redox process of O_2 in the IL, which was in agreement with previous reports. Superoxide, generated by gaining one electron at −1.2 V,[35,38−42] and peroxide anion, generated by gaining an additional electron at −1.7 V,[42−44] are quasi-reversible redox couples, as shown in Scheme 2. After adding 0.5 g of CHA/CO_2 salt into the cell (red curve), the peak current (i_p) decreased. The addition of salt may increase the viscosity of the solution, and thus, mass transport rates also decrease. Based on the Cottrell equation (1),[45] the redox current dropped consequently, as previously reported.[46,47] From the red curve of Figure 1, it is clear that the O_2^{2-} oxidation peak, around −0.3 V, disappeared, but the

https://doi.org/10.1021/acsomega.2c04748
ACS Omega 2022, 7, 42828−42834

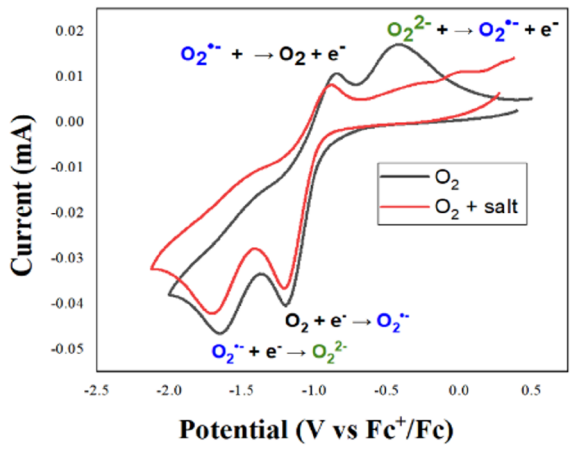

Figure 1. CV curves of pure O_2 gas in [BMIM] [NTf_2] (black curve) and with 0.5 g of the salt product from CHA and CO_2 added (red curve).

Scheme 2. Oxygen Electroreduction Reactions

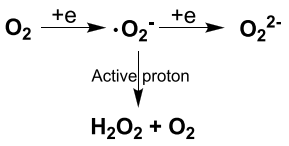

superoxide peak remained after salt was added. This suggested that O_2^{2-} was consumed in the reaction and may activate salt, while $O_2^{\bullet-}$ does not.

Based on the CV results, constant potential experiments were also performed in [BMIM] [NTf_2] and additionally in aprotic 1-butyl-1-methylpyrrolidinium bis-(trifluoromethylsulfonyl)-imide ([BMPyrr] [NTf_2]) (Figure S1). The applied potential was optimized, based on Figure 1, between −0.8 and 1.9 V. In [BMPyrr] [NTf_2], no urea was formed at potentials of −1.2 V or lower, while the highest production rate occurred around −1.6 V (Figure 2). This

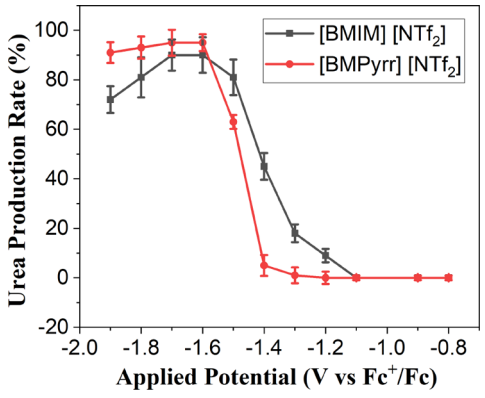

Figure 2. The production rate versus the applied potential in [BMIM] [NTf_2] and [BMPyrr] [NTf_2] at a conventional Au electrode for 5 h.

implied the two-electron oxygen reduction product, peroxide, rather than superoxide, may trigger reaction (2) (Scheme 1), converting the salt product into urea. In [BMIM] [NTf_2], a low production rate was found at −1.2 V. This may have been due to a disproportionation reaction between superoxide and the active proton in the solvent, producing O_2 and H_2O_2 as reported in other studies.[48−51] The production rates between −1.4 and −2.0 V increased accordingly with the formation of peroxide in [BMIM] [NTf_2].

Furthermore, we have characterized the compositions of salts and subsequent electrochemical products by NMR spectroscopy and FTIR spectroscopy (see Figures S2−S34). The ^{13}C NMR spectrum of the salt formed from CHA and CO_2 in [BMIM] [NTf_2] ($CDCl_3$, 25 °C, 200 MHz) is shown in Figure S4. Based on the chemical environment, the signal peak at 162 ppm was assigned to the characteristic peak of the carbamate carbonyl carbon (C=O). The C−N carbon of the ammonium and the carbamate ions in C_6H_{11}-NH_3^+:C_6H_{11}-NH-CO_2^- were responsible for the peaks at 34.53 and 33.96 ppm, respectively. After introducing oxygen gas and electrochemical potential at −1.9 V for 5 h, only one peak at 34.39 ppm was observed (Figure S2). This indicated that a product with a symmetrical structure, $(R\text{-}NH)_2CO$, was produced. Negligible double peaks from the salt were present in the NMR spectra of the final products, which implied that a high yield of salt−urea conversion was achieved. The FTIR spectrum (Figure S32) of the final products using the same starting reagents displayed the characteristic peak of urea at 1628 cm^{-1} and was attributable to the C=O stretching frequency in the N−CO−N structure (blue curve). An identical peak was also observed in an authentic dicyclohexylurea (DCU)-saturated [BMIM] [NTf_2] solution (green curve). This peak was negligible in the carbamate salt structure (red curve). The results confirmed the formation of DCU synthesized through an electrochemical process starting with CO_2 and O_2 gases. Similar results were obtained from cyclopentylamine (CPA). It should also be emphasized that no detectable byproducts were observed in the NMR and FTIR measurements in either IL.

Additional control experiments were performed using sodium peroxide (Na_2O_2) with CHA and CO_2 in [BMPyrr] [NTf_2]. The product and salt structures were characterized using ^{13}C NMR and FTIR (Figures S33−S36). The results were identical to those obtained using the same amine and IL with O_2 and CO_2 gases and applied potential. The production rate for this reaction method was determined to be 13.7%. The low production was most likely due to the extremely low solubility of Na_2O_2 in the IL,[52,53] which could hinder the catalyst effect. Further, the low solubility made extracting pure urea product from the mixture nearly impossible. For these reasons, activating the reaction electrochemically may be considered the superior method since a high conversion yield was achieved (the peroxide anion was completely soluble in this case), and product removal was easy.

The same procedure was repeated by replacing CO_2 gas with $^{13}CO_2$ gas to further confirm the reaction pathway and the formation of the urea structure. The NMR spectra were obtained in the [BMIM] [NTf_2] system (see Figures S37 and S38a,b). The ^{13}C urea product was observed at 159.23 ppm, while the ^{12}C product peak was present at 159.30 ppm. According to Lambert and Greifenstein, an isotopic shift of 0.05−0.1 ppm for $^{12}C \rightarrow {}^{13}C$ is typically seen.[54,55] Here, hydrogen-bonding and increasing bond length and angle (118° for the N−C−N angle in 1,3-dicyclohexylurea) may all contribute to an increased downfield shift, while the direction of the shift may also depend on the compound itself and the solvent used.[56,57] These NMR results confirmed that the carbonyl carbon was derived from CO_2.

Additionally, a control reaction was performed using the standard procedure, but excess CO_2 was eliminated prior to bubbling O_2 into the mixture. No urea production was

https://doi.org/10.1021/acsomega.2c04748
ACS Omega 2022, 7, 42828−42834

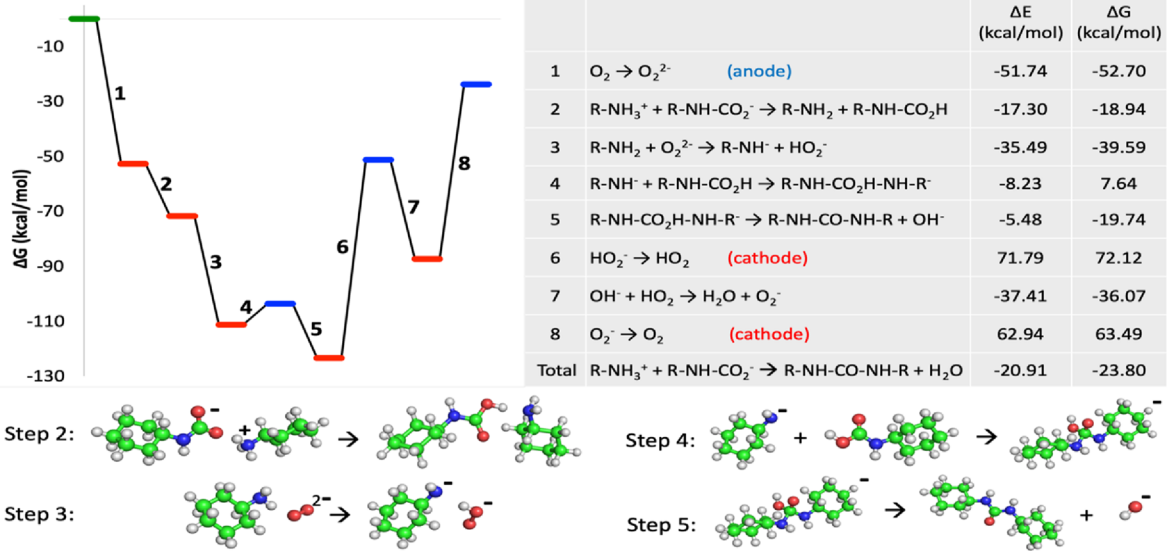

		ΔE (kcal/mol)	ΔG (kcal/mol)
1	$O_2 \rightarrow O_2^{2-}$ (anode)	-51.74	-52.70
2	$R\text{-}NH_3^+ + R\text{-}NH\text{-}CO_2^- \rightarrow R\text{-}NH_2 + R\text{-}NH\text{-}CO_2H$	-17.30	-18.94
3	$R\text{-}NH_2 + O_2^{2-} \rightarrow R\text{-}NH^- + HO_2^-$	-35.49	-39.59
4	$R\text{-}NH^- + R\text{-}NH\text{-}CO_2H \rightarrow R\text{-}NH\text{-}CO_2H\text{-}NH\text{-}R^-$	-8.23	7.64
5	$R\text{-}NH\text{-}CO_2H\text{-}NH\text{-}R^- \rightarrow R\text{-}NH\text{-}CO\text{-}NH\text{-}R + OH^-$	-5.48	-19.74
6	$HO_2^- \rightarrow HO_2$ (cathode)	71.79	72.12
7	$OH^- + HO_2 \rightarrow H_2O + O_2^-$	-37.41	-36.07
8	$O_2^- \rightarrow O_2$ (cathode)	62.94	63.49
Total	$R\text{-}NH_3^+ + R\text{-}NH\text{-}CO_2^- \rightarrow R\text{-}NH\text{-}CO\text{-}NH\text{-}R + H_2O$	-20.91	-23.80

Figure 3. Gibbs energy diagram for steps involved in the reaction R-NH_3^+ + R-NH-CO_2- → R-NH-CO-NH-R + H_2O (top left). Electronic and Gibbs energies for each step in the mechanism (top right). Molecular structure diagrams for reaction steps.

observed. This indicated that excess CO_2 might have another role in this reaction. It may react with the peroxide anion to form peroxide carbonate derivatives that would be protonated by the ammonium ions from the carbamate salts, which would generate hydroperoxide carbonate. However, no related product peaks were found in the NMR or FTIR spectra. Considering that our results agree well with previous work, we could conclude that the carbonyl carbon is in fact provided by CO_2, rather than an amine.[58]

To investigate the mechanism even further, we have performed DFT calculations of reactions relevant to this process. Figure 3 gives the proposed mechanism, along with calculated electronic and Gibbs energies for steps along the path in the formation of DCU (and water) from CHA and CO_2. Here, the reduction of oxygen gas to peroxide anion on the cathode, along with re-oxidation steps, resulting in the restoration of oxygen gas on the anode, is also included. It is seen that steps involving the reduction of dissolved O_2 and those associated with re-oxidation of HO_2^- to HO_2 and O_2^- to O_2 represent the largest shifts in energy (either free or electronic) with the reduction being favorable (ΔG = −52.70 kcal/mol) and oxidation having an energy penalty (ΔG = +135.61 kcal/mol for steps 6 and 8 combined). For steps 2−5, representing reactions directly involved with the conversion of the C_6H_{11}-NH_3^+:C_6H_{11}-NH-CO_2^- salt to $(C_6H_{11}\text{-}NH)_2CO$, electronic energy shifts are favorable for each step (the overall energy change is ΔE = −66.50 kcal/mol). The overall change in the Gibbs energy for steps 2−5 is favorable (ΔG = −70.63 kcal/mol). However, one of these steps, step 4, is associated with a relatively small energy penalty of 7.64 kcal/mol. It is likely that steps 4 and 5 in this mechanism are concerted steps, with the hydroxyl group leaving the cyclohexylcarbamic acid, while the C−N bond, resulting in urea formation, is established. The Gibbs energy change for the combination of steps 4 and 5 is −12.10 kcal/mol, which may vary with the steric effect of different amines.

To study how generally this method can be applied, the same procedure was repeated with various amines in [BMIM] [NTf_2] (Figures S5−S24) and [BMPyrr] [NTf_2] (Figures S25−S31). The NMR results, as shown in Figures S2−S19, indicate that CHA, CPA, and linear amines all form urea structures in [BMIM] [NTf_2]. Branched amines yield little or no product; aniline also failed to generate the product (Figures S20−S24). The results were consistent with previous work.[59] However, the reasons for the diminished reactivities are not known but are thought to be related to modified electronic properties of NH_2 groups relative to linear amines, CHA, and CPA. Reduced reactivity might be attributable either to reduced participation in the urea formation reactions themselves or to variations in the solubilities of the R-NH_3^+:R-NH-COO^- salts. Interestingly, both dipropylamine and dihexylamine reacted to form significant yields of $(R_2\text{-}N)_2CO$ ureas when [BMPyrr] [NTf_2] was the solvent. The percent conversion and turnover frequencies (TOF) were determined without CO_2 recycling and are given in Table 1.

Table 1. Percent Conversion and Turnover Frequencies of Various Amines

amines	% conv. in [BMIM] [NTf_2]	TOF (s^{-1}) in [BMIM] [NTf_2]	% conv. in [BMPyrr] [NTf_2]	TOF (s^{-1}) in [BMPyrr] [NTf_2]
cyclohexylamine	88	78.411	93	108.44
CHA/sodium peroxide	N/A	N/A	13.7	N/A
cyclopentylamine	86	36.21	90	35.98
pentylamine	87	208.91	90	6.26
hexylamine	65	88.00	76	16.28
heptylamine	46	12.86	49	147.48
octylamine	14	10.03	22.5	73.46
dihexylamine	7	86.73	30	218.25
dipropylamine	5	N/A	43	N/A
piperidine	0	N/A	0	N/A

The results were largely consistent with the NMR (and FTIR) results discussed above. Reaction yields in the two ILs are seen to vary substantially for different amine reactants. It showed more than 90% conversion rate for CHA, CPA, and pentylamine in [BMPyrr] [NTf_2] and decreased with increasing carbon chain length, which may be due to the steric effect mentioned previously. For amines with more than

https://doi.org/10.1021/acsomega.2c04748
ACS Omega 2022, 7, 42828−42834

eight carbons, conversion rates dropped to lower than 22.5%. However, amines demonstrating high urea yields through this reaction covered the most common ureas available. The reasons for this are not completely understood. One factor could be the presence of a protic or aprotic cation in the IL. The [BMPyrr] cation has a tendency to promote the stability of the peroxide dianion to a greater extent than the protic [BMIM] cation.[60,61] It is also possible that the IL cation directly affects the solubility of the R-NH_3^+:R-NH-COO^- salt, indirectly affecting reaction yields.

A spectroelectrochemical cell from Bio-Logic was used to measure the formation of urea in situ as reported in other systems.[58,62] The spectra were recorded every 10 min starting from pure [BMIM] [NTf_2] (Figure 4). After 20 min, 10 μL of

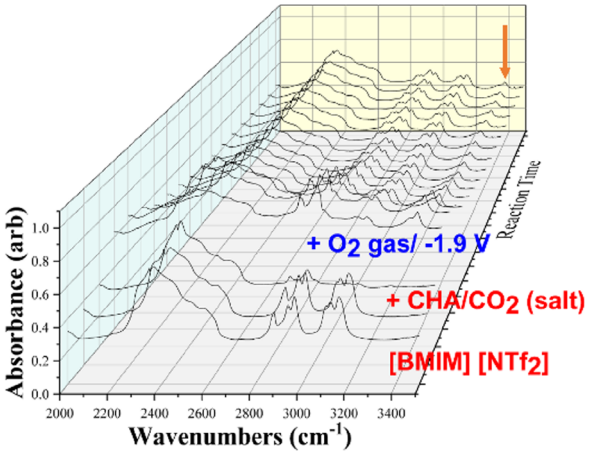

Figure 4. In situ EC-FTIR measurements. The spectra were recorded every 10 min. The first labeled spectrum resulted from pure [BMIM] [NTf_2]. CHA and CO_2 were added at 20 min (third curve). The fourth spectrum was recorded after 10 min of applying O_2 gas and −1.9 V.

CHA was added with CO_2 purging for 5 min. The signals of the spectrum became lower since the solid salt instantly formed while being suspended in the IL. Then, O_2 gas was purged into the system with a constant potential of −1.9 V applied for the entirety of the EC experiment. A new peak was observed at 3386 cm^{-1}, which was attributed to the N−H stretching in 1,3-dicyclohexylurea.[63,64] With time, the peak stopped increasing, which implied quick saturation due to the low solubility of urea. Moreover, the stability of [BMIM] [NTf_2] as the sole electrolyte and solvent was investigated. The EC reaction was monitored over 7 h with a continuously applied potential of −1.9 V. From our results, the IL peaks remained unchanged throughout the experiments, demonstrating its excellent stability. The structural stability was also confirmed by ^{1}H NMR measurements of the [BMIM] [NTf_2] before and after the reaction (see Figure S39a,b).

In conclusion, we have developed a highly selective, efficient, safe, and inexpensive method for synthesizing C−N compounds, which can be performed at ambiance within a short time. Unlike previously reported techniques, no external catalysts nor reagents other than oxygen gas are needed, and special modification or preparation of the electrode surface is not required. The most accessible amines on the market can be used to generate short carbon chain urea with more than 92% production. The concept of such a catalyst system could be expanded to other fields and exploited industrially.

■ ASSOCIATED CONTENT

Supporting Information

The Supporting Information is available free of charge at https://pubs.acs.org/doi/10.1021/acsomega.2c04748.

Experimental details, computations, ^{13}C NMR spectra of all compounds, and FTIR spectra of selected compounds (PDF)

■ AUTHOR INFORMATION

Corresponding Author

Zhe Wang − *Department of Chemistry, Oakland University, Rochester, Michigan 48309, United States;* orcid.org/0000-0003-3762-3167; Email: zhewang@oakland.edu

Authors

Erin Witherspoon − *Department of Chemistry, Oakland University, Rochester, Michigan 48309, United States*

Pinghua Ling − *Department of Chemistry, Xavier University of Louisiana, New Orleans, Louisiana 70125, United States*

William Winchester − *Department of Chemistry, Oakland University, Rochester, Michigan 48309, United States*

Qi Zhao − *Department of Chemistry, Tulane University, New Orleans, Louisiana 70118, United States*

Ahmad Ibrahim − *Department of Chemistry, Oakland University, Rochester, Michigan 48309, United States*

Kevin E. Riley − *Department of Chemistry, Xavier University of Louisiana, New Orleans, Louisiana 70125, United States*

Complete contact information is available at: https://pubs.acs.org/10.1021/acsomega.2c04748

Notes

The authors declare no competing financial interest.

■ ACKNOWLEDGMENTS

This publication was made possible by the support from the Army Research Office under grant number W911NF-18-1-0458 and the National Science Foundation (CHE-1832167, HRD-1700429, and HRD-1505219).

■ REFERENCES

(1) Houlton, B. Z.; Almaraz, M.; Aneja, V.; Austin, A. T.; Bai, E.; Cassman, K. G.; Compton, J. E.; Davidson, E. A.; Erisman, J. W.; Galloway, J. N.; Gu, B.; Yao, G.; Martinelli, L. A.; Scow, K.; Schlesinger, W. H.; Tomich, T. P.; Wang, C.; Zhang, X. A World of Cobenefits: Solving the Global Nitrogen Challenge. *Earth's Future* **2019**, *7*, 865−872.

(2) Nations, F. a. A. O. o. t. U., *World fertilizer trends and outlook to 2022.*; Food and Agriculture Organization of the United Nations: 2019.

(3) Ghosh, A. K.; Brindisi, M. Urea Derivatives in Modern Drug Discovery and Medicinal Chemistry. *J. Med. Chem.* **2020**, *63*, 2751−2788.

(4) Shirvan, A. R.; Shakeri, M.; Bashari, A., Recent advances in application of chitosan and its derivatives in functional finishing of textiles. in *The impact and prospects of green chemistry for textile technology*; Woodhead Publishing, 2019, 107−133.

(5) Atashkar, B.; Zolfigol, M. A.; Mallakpour, S. Applications of biological urea-based catalysts in chemical processes. *Mol. Cata.* **2018**, *452*, 192−246.

(6) Li, H.-Q.; Lv, P.-C.; Yan, T.; Zhu, H.-L. Urea derivatives as anticancer agents. *Anti-Cancer Agents Med. Chem.* **2009**, *9*, 471−480.

(7) Yokoya, M.; Kimura, S.; Yamanaka, M. Urea derivatives as functional molecules: supramolecular capsules, supramolecular

polymers, supramolecular gels, artificial hosts, and catalysts. *Chem. - Eur. J.* **2021**, *27*, 5601−5614.
(8) Amendola, V.; Fabbrizzi, L.; Mosca, L. Anion recognition by hydrogen bonding: urea-based receptors. *Chem. Soc. Rev.* **2010**, *39*, 3889−3915.
(9) Song, E. Y.; Kaur, N.; Park, M.-Y.; Jin, Y.; Lee, K.; Kim, G.; Lee, K. Y.; Yang, J. S.; Shin, J. H.; Nam, K.-Y.; No, K. T.; Han, G. Synthesis of amide and urea derivatives of benzothiazole as Raf-1 inhibitor. *Eur. J. Med. Chem.* **2008**, *43*, 1519−1524.
(10) Meessen, J. Urea synthesis. *Chem. Ing. Tech.* **2014**, *86*, 2180−2189.
(11) Wu, C.; Cheng, H.; Liu, R.; Wang, Q.; Hao, Y.; Yu, Y.; Zhao, F. Synthesis of urea derivatives from amines and CO_2 in the absence of catalyst and solvent. *Green Chem.* **2010**, *12*, 1811−1816.
(12) Xu, M.; Jupp, A. R.; Ong, M. S.; Burton, K. I.; Chitnis, S. S.; Stephan, D. W. Synthesis of urea derivatives from CO_2 and silylamines. *Am. Ethnol.* **2019**, *131*, 5763−5767.
(13) Lv, C.; Zhong, L.; Liu, H.; Fang, Z.; Yan, C.; Chen, M.; Kong, Y.; Lee, C.; Liu, D.; Li, S.; Liu, J.; Song, L.; Chen, G.; Yan, Q.; Yu, G. Selective electrocatalytic synthesis of urea with nitrate and carbon dioxide. *Nat. Sustainable* **2021**, *4*, 868−876.
(14) Wang, H.; Xin, Z.; Li, Y., Synthesis of Ureas from CO_2. *Chemical Transformations of Carbon Dioxide*; Springer 2017, 177−202, DOI: 10.1007/978-3-319-77757-3_5.
(15) Zhu, X.; Zhou, X.; Jing, Y.; Li, Y. Electrochemical synthesis of urea on MBenes. *Nat. Commun.* **2021**, *12*, 4080.
(16) Yuan, M.; Chen, J.; Bai, Y.; Liu, Z.; Zhang, J.; Zhao, T.; Shi, Q.; Li, S.; Wang, X.; Zhang, G. Electrochemical C−N coupling with perovskite hybrids toward efficient urea synthesis. *Chem. Sci.* **2021**, *12*, 6048−6058.
(17) Centi, G.; Quadrelli, E. A.; Perathoner, S. Catalysis for CO 2 conversion: a key technology for rapid introduction of renewable energy in the value chain of chemical industries. *Energy Environ. Sci.* **2013**, *6*, 1711−1731.
(18) Sakakura, T.; Choi, J.-C.; Yasuda, H. Transformation of carbon dioxide. *Chem. Rev.* **2007**, *107*, 2365−2387.
(19) Rakowski Dubois, M.; Dubois, D. L. Development of molecular electrocatalysts for CO_2 reduction and H_2 production/oxidation. *Acc. Chem. Res.* **2009**, *42*, 1974−1982.
(20) Aresta, M.; Dibenedetto, A.; Angelini, A. Catalysis for the valorization of exhaust carbon: from CO_2 to chemicals, materials, and fuels. Technological use of CO_2. *Chem. Rev.* **2014**, *114*, 1709−1742.
(21) Benson, E. E.; Kubiak, C. P.; Sathrum, A. J.; Smieja, J. M. Electrocatalytic and homogeneous approaches to conversion of CO_2 to liquid fuels. *Chem. Soc. Rev.* **2009**, *38*, 89−99.
(22) Peterson, A. A.; Abild-Pedersen, F.; Studt, F.; Rossmeisl, J.; Nørskov, J. K. How copper catalyzes the electroreduction of carbon dioxide into hydrocarbon fuels. *Energy Environ. Sci.* **2010**, *3*, 1311−1315.
(23) Marcos, M. L.; González-Velasco, J.; Bolzán, A. E.; Arvia, A. J. Comparative electrochemical behaviour of CO_2 on Pt and Rh electrodes in acid solution. *J. Electroanal. Chem.* **1995**, *395*, 91−98.
(24) Lim, R. J.; Xie, M.; Sk, M. A.; Lee, J.-M.; Fisher, A.; Wang, X.; Lim, K. H. A review on the electrochemical reduction of CO_2 in fuel cells, metal electrodes and molecular catalysts. *Catal. Today* **2014**, *233*, 169−180.
(25) Ma, F.-X.; Wang, J.; Wang, F.-B.; Xia, X.-H. The room temperature electrochemical synthesis of N-doped graphene and its electrocatalytic activity for oxygen reduction. *Chem. Commun.* **2015**, *51*, 1198−1201.
(26) Shibata, M.; Furuya, N. Electrochemical synthesis of urea at gas-diffusion electrodes: Part VI. Simultaneous reduction of carbon dioxide and nitrite ions with various metallophthalocyanine catalysts. *J. Electroanal. Chem.* **2001**, *507*, 177−184.
(27) Shibata, M.; Yoshida, K.; Furuya, N. Electrochemical Synthesis of Urea at Gas-Diffusion Electrodes: IV. Simultaneous Reduction of Carbon Dioxide and Nitrate Ions with Various Metal Catalysts. *J. Electroanal. Chem.* **1998**, *145*, 2348.
(28) da Silva Freitas, W.; D'Epifanio, A.; Mecheri, B. Electrocatalytic CO2 reduction on nanostructured metal-based materials: Challenges and constraints for a sustainable pathway to decarbonization. *J. CO2 Util.* **2021**, *50*, No. 101579.
(29) Phan, Q. T.; Poon, K. C.; Sato, H. A review on amorphous noble-metal-based electrocatalysts for fuel cells: Synthesis, characterization, performance, and future perspective. *Int. J. Hydrogen Energy* **2021**, *46*, 14190−14211.
(30) Manaka, Y.; Nagatsuka, Y.; Motokura, K. Organic bases catalyze the synthesis of urea from ammonium salts derived from recovered environmental ammonia. *Sci. Rep.* **2020**, *10*, 2834.
(31) Ohno, H., *Electrochemical aspects of ionic liquids*; John Wiley & Sons: 2005.
(32) Armand, M.; Endres, F.; MacFarlane, D. R.; Ohno, H.; Scrosati, B., Ionic-liquid materials for the electrochemical challenges of the future. *Materials for sustainable energy: a collection of peer-reviewed research and review articles from Nature Publishing Group*; World Scientific: 2011, 129−137.
(33) Wang, Z.; Kumar, A.; Sevilla, M. D.; Zeng, X. Anaerobic Oxidation of Methane to Methyl Radical in NTf2-Based Ionic Liquids. *J. Phys. Chem. C* **2016**, *120*, 13466−13473.
(34) Tang, Y.; Wang, Z.; Chi, X.; Sevilla, M. D.; Zeng, X. *In Situ* Generated Platinum Catalyst for Methanol Oxidation via Electrochemical Oxidation of Bis(trifluoromethylsulfonyl)imide Anion in Ionic Liquids at Anaerobic Condition. *J. Phys. Chem. C* **2016**, *120*, 1004−1012.
(35) Wang, Z.; Lin, P.; Baker, G. A.; Stetter, J.; Zeng, X. Ionic liquids as electrolytes for the development of a robust amperometric oxygen sensor. *Anal. Chem.* **2011**, *83*, 7066−7073.
(36) Villagrán, C.; Aldous, L.; Lagunas, M. C.; Compton, R. G.; Hardacre, C. Electrochemistry of phenol in bis {(trifluoromethyl) sulfonyl} amide ([NTf2]−) based ionic liquids. *J. Electroanal. Chem.* **2006**, *588*, 27−31.
(37) Gondosiswanto, R.; Hibbert, D. B.; Fang, Y.; Zhao, C. Ionic liquid microstrips impregnated with magnetic nanostirrers for sensitive gas sensors. *ACS Appl. Mater. Interfaces* **2017**, *9*, 43377−43385.
(38) Wang, Z.; Zeng, X. Bis (trifluoromethylsulfonyl) imide (NTf2)-based ionic liquids for facile methane electro-oxidation on Pt. *J. Electroanal. Chem.* **2013**, *160*, H604.
(39) Hayyan, M.; Hashim, M. A.; AlNashef, I. M. Superoxide ion: generation and chemical implications. *Chem. Rev.* **2016**, *116*, 3029−3085.
(40) Hayyan, M.; Mjalli, F. S.; AlNashef, I. M.; Hashim, M. A. Chemical and electrochemical generation of superoxide ion in 1-butyl-1-methylpyrrolidinium bis (trifluoromethylsulfonyl) imide. *Int. J. Electrochem. Sci.* **2012**, *7*, 8116−8127.
(41) Khan, A.; Gunawan, C. A.; Zhao, C. Oxygen reduction reaction in ionic liquids: fundamentals and applications in energy and sensors. *ACS Sustainable Chem. Eng.* **2017**, *5*, 3698−3715.
(42) Pozo-Gonzalo, C., Oxygen reduction reaction in ionic liquids: an overview. In: Torriero, A. (eds) *Electrochemistry in Ionic Liquids*; Springer: Cham. 2015, 507−529.
(43) Zhang, Y.; Pozo-Gonzalo, C. Variations and applications of the oxygen reduction reaction in ionic liquids. *Chem. Commun.* **2018**, *54*, 3800−3810.
(44) De Giorgio, F.; Soavi, F.; Mastragostino, M. Effect of lithium ions on oxygen reduction in ionic liquid-based electrolytes. *Electrochem. Commun.* **2011**, *13*, 1090−1093.
(45) Bard, A. J.; Faulkner, L. R., *Electrochemical Methods: Fundamentals and Applications, 2nd Edition*; John Wiley & Sons, Incorporated: 2000.
(46) Tomcsányi, L.; De Battisti, A.; Hirschberg, G.; Varga, K.; Liszi, J. The study of the electrooxidation of chloride at RuO2/TiO2 electrode using CV and radiotracer techniques and evaluating by electrochemical kinetic simulation methods. *Electrochim. Acta* **1999**, *44*, 2463−2472.

https://doi.org/10.1021/acsomega.2c04748
ACS Omega 2022, 7, 42828−42834

(47) Bott, A. W. Characterization of chemical reactions coupled to electron transfer reactions using cyclic voltammetry. *Curr. Sep.* **1999**, *18*, 9−16.
(48) Khan, A.; Lu, X.; Aldous, L.; Zhao, C. Oxygen reduction reaction in room temperature protic ionic liquids. *J. Phys. Chem. C* **2013**, *117*, 18334−18342.
(49) Switzer, E. E.; Zeller, R.; Chen, Q.; Sieradzki, K.; Buttry, D. A.; Friesen, C. Oxygen reduction reaction in ionic liquids: The addition of protic species. *J. Phys. Chem. C* **2013**, *117*, 8683−8690.
(50) Pozo-Gonzalo, C.; Torriero, A. A. J.; Forsyth, M.; MacFarlane, D. R.; Howlett, P. C. Redox chemistry of the superoxide ion in a phosphonium-based ionic liquid in the presence of water. *J. Phys. Chem. Lett.* **2013**, *4*, 1834−1837.
(51) Sawyer, D. T., In *Oxygen chemistry*; Oxford university press: 1991; Vol. *26*.
(52) DeLand, F. H., In *CRC Handbook of Chemistry and Physics*; CRC Press, Inc., RC, West; MJ, Astle; WH, Beyer, Eds. Boca Raton, Florida, 1983, 2386
(53) Budavari, S.; O'Neil, M. J.; Smith, A.; Heckelman, P. E., In *The merck index.*; Merck Rahway: NJ: 1989; Vol. *11*.
(54) Lambert, J. B.; Greifenstein, L. G. Origin of the chemical-shift isotope effect. Stereochemical evidence. *J. Am. Chem. Soc.* **1974**, *96*, 5120−5124.
(55) Hansen, P. E., Isotope effects on nuclear shielding. In *Annual reports on NMR spectroscopy*; Elsevier: 1984; Vol. *15*, pp. 105−234, DOI: 10.1016/S0066-4103(08)60208-2.
(56) Hansen, P. E. Isotope effects on chemical shifts in the study of intramolecular hydrogen bonds. *Molecules* **2015**, *20*, 2405−2424.
(57) Vaughan, P.; Donohue, J. The structure of urea. Interatomic distances and resonance in urea and related compounds. *Acta Crystallogr.* **1952**, *5*, 530−535.
(58) Wang, J. IR spectroelectrochemical investigations of solvent roles in deactivation of poly (3-methylthiophene) films. *Electrochim. Acta* **1997**, *42*, 2545−2554.
(59) Mindrup, E. M.; Schneider, W. F. Computational comparison of the reactions of substituted amines with CO2. *ChemSusChem* **2010**, *3*, 931−938.
(60) Monaco, S.; Arangio, A. M.; Soavi, F.; Mastragostino, M.; Paillard, E.; Passerini, S. An electrochemical study of oxygen reduction in pyrrolidinium-based ionic liquids for lithium/oxygen batteries. *Electrochim. Acta* **2012**, *83*, 94−104.
(61) Hayyan, M.; Mjalli, F. S.; Hashim, M. A.; AlNashef, I. M.; Al-Zahrani, S. M.; Chooi, K. L. Long term stability of superoxide ion in piperidinium, pyrrolidinium and phosphonium cations-based ionic liquids and its utilization in the destruction of chlorobenzenes. *J. Electroanal. Chem.* **2012**, *664*, 26−32.
(62) Hartl, F.; Luyten, H.; Nieuwenhuis, H. A.; Schoemaker, G. C. Versatile cryostated optically transparent thin-layer electrochemical (OTTLE) cell for variable-temperature UV-Vis/IR spectroelectrochemical studies. *Appl. Spectrosc.* **1994**, *48*, 1522−1528.
(63) *SpectraBase*; Wiley: 1989, 1990−2021.
(64) Rehder, S.; Sakmann, A.; Rades, T.; Leopold, C. S. Thermal degradation of amorphous glibenclamide. *Eur. J. Pharm. Biopharm.* **2012**, *80*, 203−208.

https://doi.org/10.1021/acsomega.2c04748
ACS Omega 2022, 7, 42828−42834